Filament Eruption after the Onset of the X1.5 Flare on 2005 September 13

Haimin Wang, Chang Liu, Ju Jing, and Vasyl Yurchyshyn

Big Bear Solar Observatory, New Jersey Institute of Technology, 40386 North Shore Lane, Big Bear City, CA 92314-9672, USA

haimin@flare.njit.edu - Version on March 1, 2007

ABSTRACT

Erupting filaments usually play the role as the initial driver of flaring process preceding the subsequent flare emissions. In this Letter, we report a rare case that during the X1.5 flare on 2005 September 13, a filament at the boundary of the NOAA AR 0808 erupted ∼13 minutes after the flare onset at ∼19:22 UT near the central AR neutral line. During this time period, the filament only showed a slow rising; meanwhile, a spatially associated large magnetic loop with one leg connecting to the initial flaring site began to brighten in the TRACE 195 Å channel. After ∼19:35 UT, the filament abruptly erupted together with the bright TRACE loop. Besides the moving ribbons at the first flaring site, the filament eruption caused a secondary flare identified with another set of moving ribbons. We suggest possible triggering mechanisms for the initial flare and the eruption of the peripheral flux loop system, which leads to the sympathetic flaring.

Subject headings: Sun: activity — Sun: filaments — Sun: flares — Sun: magnetic fields

1. INTRODUCTION

As more comprehensive observational and modeling tools have been developed in the past decade, it becomes clearer that flares may have complicated spatial and temporal structures, and can have wide-spread effects over the solar disk. A localized flaring process can produce remote brightenings outside flare core regions by transporting hot electrons there (Manoharan et al. 1996; Wang et al. 2002; Wang 2005; Liu 2006), and can launch a shock wave that subsequently triggers a coronal mass ejection (CME) by destabilizing large transequatorial loops (e.g., Khan & Hudson 2000). Two flares can also occur consecutively in the same or nearby active regions during a short period of time, which are thus termed sympathetic flares (Pearce & Harrison 1990; Shi, Wang & Luan 1997; Gopalswamy et al. 1999; Zhang et al. 2000; Moon et al. 2002; Wheatland & Craig

2006). The sympathy of solar flares is evidenced clearly in a number of statistical studies (e.g., Moon et al. 2002; Wheatland & Craig 2006), and naturally indicates certain physical connection between different flare sites, such as X-ray ejecta from the eruption region (Gopalswamy et al. 1999) and energy redistribution along large-scale loop via heat conduction (Zhang et al. 2000). However, the morphological demonstration in terms of physical connection of multiple events has been rare. Wang et al. (2001) studied two sympathetic M-class solar flares that erupted in succession in the NOAA AR 8869 and 8872, respectively. Authors demonstrated the loop activation, which appears to be the consequence of the first flare in AR 8869 and the cause of the second flare in AR 8872.

To probe the diverse flaring phenomena, filaments and their dynamics can be an important clue. Most of two ribbon flares can be explained reasonably by the classical Kopp-Pneuman model (Kopp & Pneuman 1976), in which the eruption of a filament (or a flux rope) opens overlying arcade fields, and successive reconnection of them causes the outward propagation of flare ribbons in the lower atmosphere. Therefore, the flare emission should follow the initiation of filament eruption. Observationally, Wang et al. (2003) demonstrated clearly the time sequence of an eruptive events: the filament eruption, flaring, and then a CME. The initial eruption of filament can be caused by loss of equilibrium such as formulated by Birn et al. (2006). On the other hand, filaments away from the flare core region can be disturbed but not disrupted, after the onset of a flare. In such a case, it implies the passage of a large-scale wave disturbance originating in a flare (e.g., Liu 2006).

In this Letter, we report a rarely observed case: a filament eruption occurred $\sim$13 minutes after the onset of the initial main flare and caused a sympathetic two ribbon flare at a different magnetic neutral line.

2. DATA SOURCES

From the Solar Geophysical Data, the X1.5 flare peaked at 19:20 UT on 2005 September 13. Full-disk Hα images were obtained at the Big Bear Solar Observatory (BBSO), with 1$''$ pixel resolution and 1 minute cadence. BBSO usually observes at the line center of Hα. On 2005 September 13, the filter was set at –0.6 Å towards blue to monitor the early signature of eruptions.

This event was covered by the Transition Region and Corona Explorer (TRACE; Handy et al. 1999). TRACE usually has a larger, but compatible field of view ($510'' \times 510''$) to that of BBSO high resolution observations ($300'' \times 300''$). For this event, TRACE observed mainly at 195 Å.

The Owens Valley Solar Array (OVSA; Gary & Hurford 1990) observed the event completely, while the Reuven Ramaty High Energy Solar Spectroscopic Imager (RHESSI; Lin et al. 2002) had

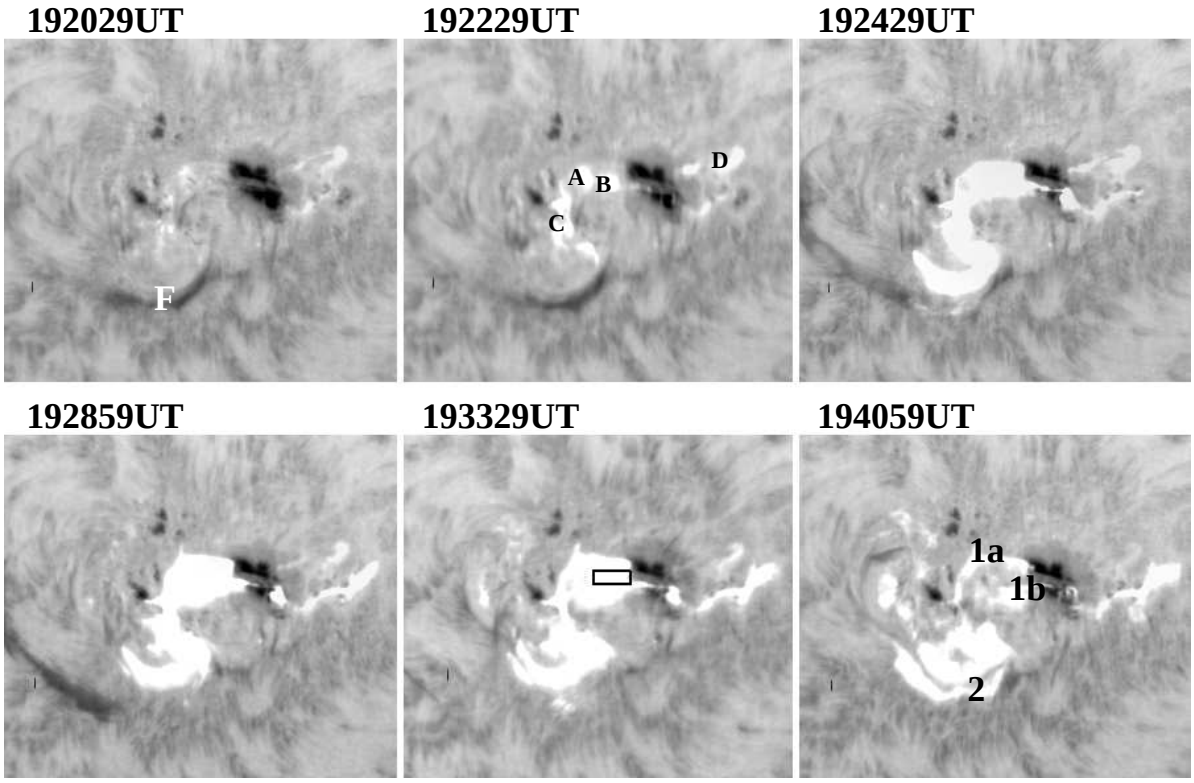

Fig. 1.— A time sequence of BBSO Hα – 0.6 Å images covering the 2005 September 13 X1.5 flare. The field of view is $300'' \times 260''$. F is the erupting filament at the boundary of the AR. A, B, C and D are four initial flaring footpoints. 1*a*, 1*b* and 2 are three moving ribbons. The black box marked a section of magnetic neutral line that will be discussed in Figure 5.

a partial coverage. These observations reveal the properties of accelerated electrons in addition to their spatial and temporal distribution.

In addition, vector magnetograms were obtained from around 17 UT to beyond 24 UT by BBSO's Digital Vector Magnetograph (DVMG) system. The hardware was described in detail by Spirock et al. (2002). Each data set consists of four images: a 6103 Å filtergram (Stokes-I), a line-of-sight magnetogram (Stokes-V), and the transverse magnetograms (Stokes-U and -Q). We re-bin the camera to the 512×512 mode to increase the sensitivity of the magnetograms. After rebinning, the pixel resolution is about $0.6''$. The line-of-sight magnetic sensitivity is approximately 2 Gauss while the transverse magnetic sensitivity is approximately 20 Gauss. The cadence for a complete set of Stokes images is 1 minute.

3. OBSERVATIONAL FINDINGS

Figure 1 shows a sequence of Hα off-band filtergrams. The filament at the boundary of the AR is marked as F at 19:20 UT. The initiation of the flare occurred at $\sim$19:22 UT, when four main Hα kernels marked as A, B, C, and D can be distinguished. The comparison between this frame with the co-temporal MDI longitudinal magnetogram (see Figure 2) shows that A and C have positive polarity while B and D have negative polarity. In two minutes, the flare evolves rapidly to the main phase, with the flare kernel C extending southward to form a shape of a letter S. Coinciding with the impulsive phase of the flare, a pair of separating ribbons 1*a* and 1*b*, which originated from the initial flare kernels A and B, respectively, is identified. The position of the front of these two ribbons are plotted in Figure 3 (upper two panels). Same as what described in Wang et al. (2003), the ribbon separation has two phases, a fast one followed by a slow one. Based on linear fitting, the speeds of ribbon 1*a* are 28.7 km/s in the first phase, and 2.1 km/s in the second phase. The speeds of ribbon 1*b* are 16.4 km/s and 0.3 km/s, respectively.

We use RHESSI images to further understand the magnetic topology of the initial flaring. RHESSI entered night time at $\sim$19:20:30 UT before the flare impulsive phase peaked at $\sim$19:27 UT. Figure 2 shows the RHESSI X-ray loops in the 6–12 keV reconstructed using grids 3–8 in the early phase of the flare at $\sim$19:20 UT, over-plotted onto a BBSO Hα off-band image showing the initial brightening of the four main Hα kernels. A comparison with a magnetogram is also included. Mapping at this low energy usually shows the sources of loop top. The connectivity between Hα kernels B and C is quite obvious, while we can vaguely identify the connectivity between A and D. AD connection has been more clearly identified by Non-Linear Force-Free extrapolation that will be presented in a separate paper. As these were observed at the beginning of the flare, they are the signature of initial heating of the flaring process. This may support one of our main points that the flare was triggered due to the interaction of loops BC and AD. However, no hard X-ray footpoint sources related to all the Hα kernels are found due to the low counts of hard X-rays at this time.

As we stated earlier, typically, a filament starts to erupt prior to the peak of the main flare (e.g., Wang et al. 2003). In this event, the filament (labeled as F in Fig. 1) started to rise *after* the initial flare brightenings, and the eruption took place at $\sim$19:35 UT, not associated with the impulsive phase of the main flare that is corresponding to the ribbon separation of 1*a* and 1*b*. In the bottom panel of Figure 3, we plot the filament height as a function of time based on both BBSO and TRACE observations. To correct the projection, we assume that the eruption is normal to the solar surface. The results of linear fitting show that the filament first slowly rose at a speed of 129 km/s and transited to the rapid eruption phase with a speed of 402 km/s. Immediately after the take-off the filament, another moving ribbon 2 is identified (see Fig. 1). The conjugate ribbon for 2 is buried in the already brightened flare patch C and is discernible in a time-lapse movie. Nevertheless, since the speeds of the moving ribbon 2 are 46.2 km/s then 6.2 km/s, with

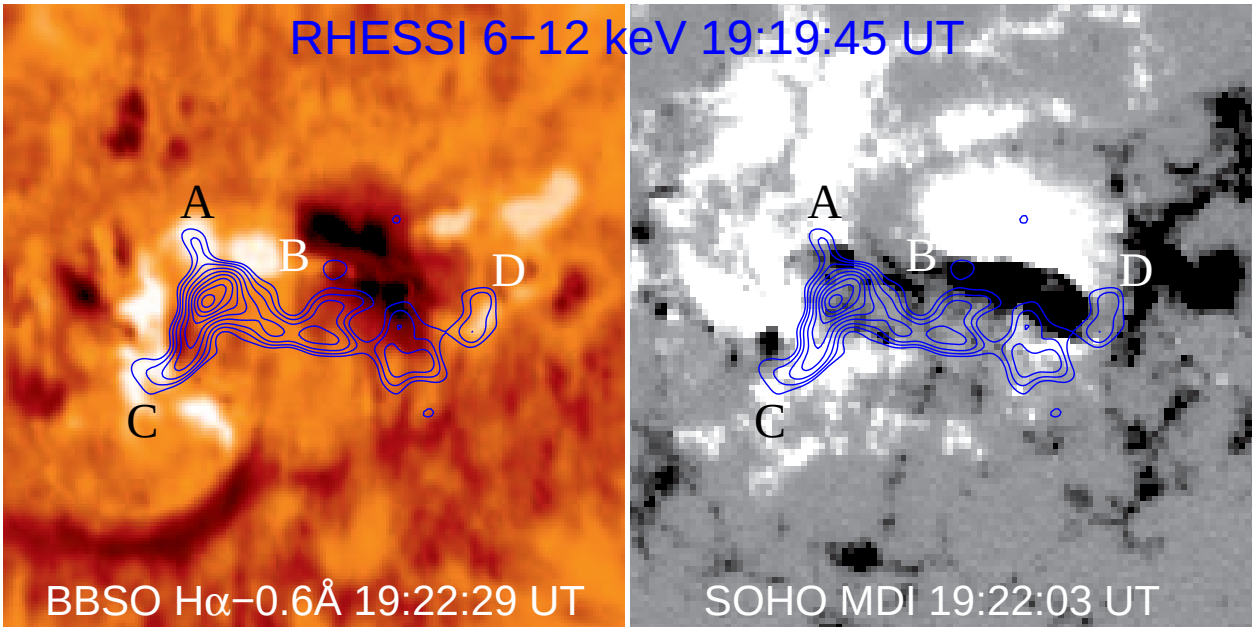

Fig. 2.— X-ray flare loop observation in the early phase of the 2005 September 13 X1.5 flare. RHESSI 6–12 keV X-ray contours (blue) are superimposed on a BBSO Hα – 0.6 Å image taken at 19:22:29 UT (*left*) and a SOHO MDI magnetogram at 19:22:03 UT (*right*). A, B, C, and D are four initial Hα flare kernels. A and C have positive polarity, while B and D have negative polarity. The RHESSI image was reconstructed for the period 19:19:00–19:20:30 UT using the CLEAN algorithm with a spatial resolution of $\sim$9.7″ FWHM. The shown contour levels are 22%, 28%, 35%, 45%, 55%, 65%, 75%, 85%, and 95% of the maximum.

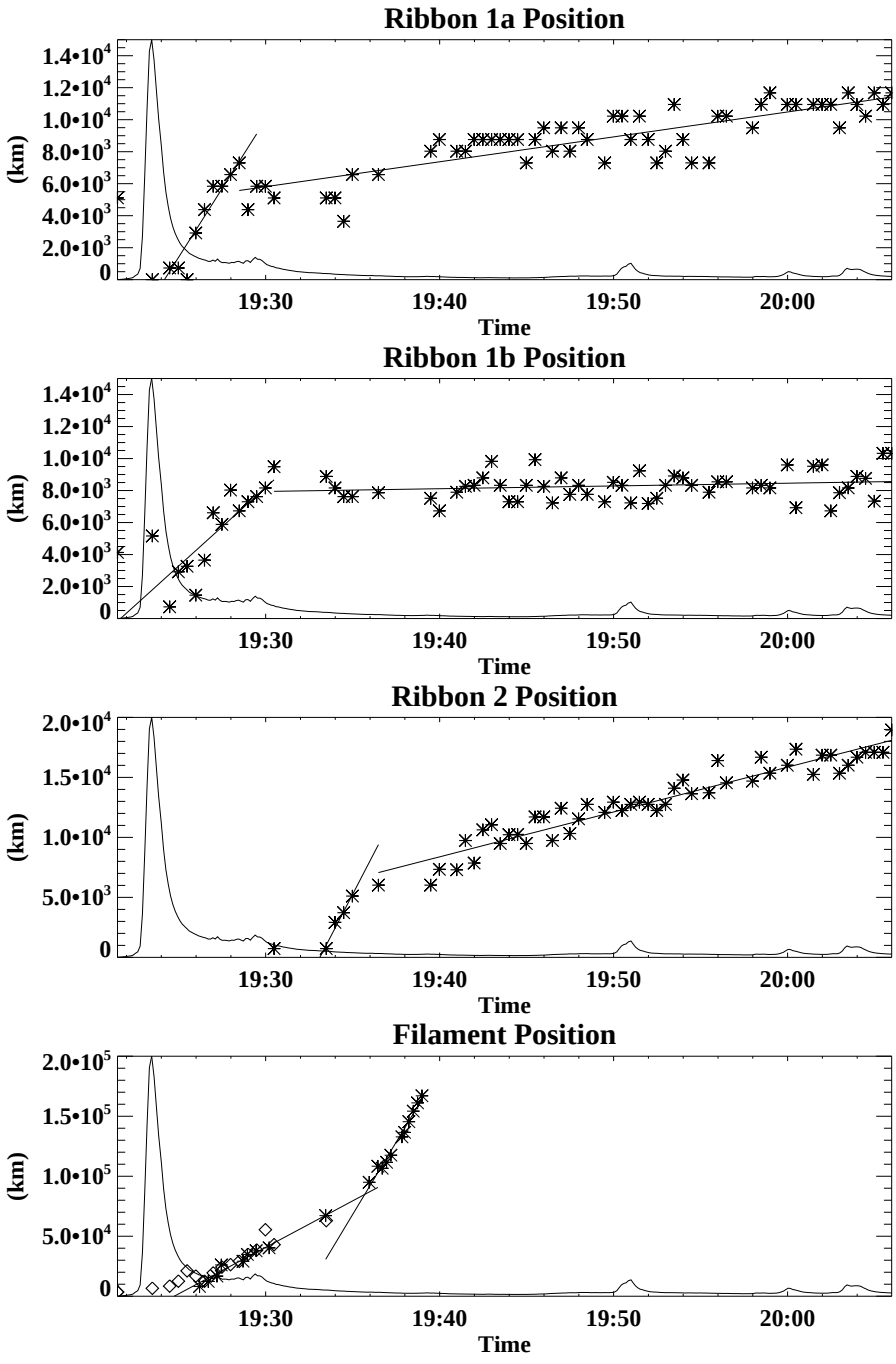

Fig. 3.— The position of front of the three moving flare ribbons as a function of time. The solid line is the light curve of microwave at 10 GHz observed by OVSA. The bottom panel shows the filament heights. Diamonds are points based on BBSO Hα observations, while the stars are based on TRACE 195 Å observations. Straight lines are fittings to derive speeds of motions.

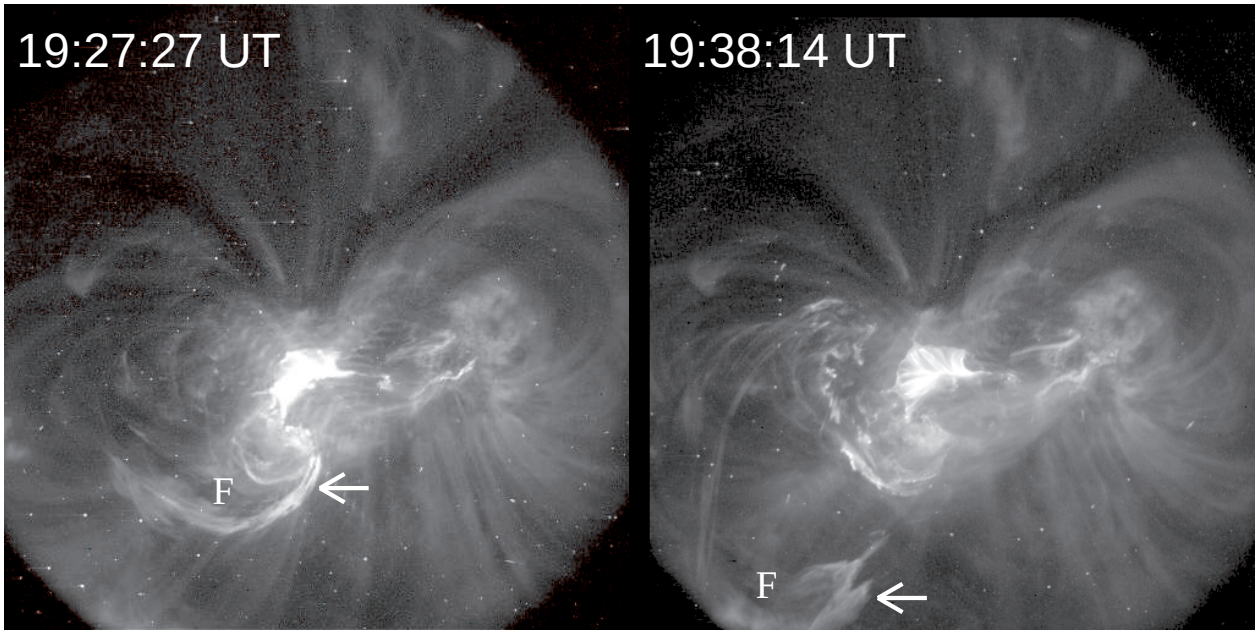

Fig. 4.— TRACE 195 Å images showing the brightening of a large loop (denoted by arrow), which is co-spatial with the filament ("F"), following the initial flaring and its final eruption after ∼19:35 UT.

the fast phase coinciding with the rapid eruption of the filament, it represents the reconnection as a consequence of the moving filament cutting through the arcade fields. Moreover, the filament runs along a neutral line different from the location of the initial flaring. Therefore, we identified both temporally and spatially that the filament eruption is not the cause of but triggered by the main event. Because the moving ribbons 2 and 1a-1b are spatially linked via flare patch C and happened within a short time period, they are considered as sympathetic flares.

As to how the initial flaring triggered the filament eruption and subsequent sympathetic flare, the TRACE EUV movie reveals an unique process that is related to this question. The filament as well as the co-spatial bright TRACE loops can be seen in the preflare state southeast of the TRACE field of view. At 19:24 UT southern ends of large-scale loops are brightened in the vicinity of the S-shaped flare patch C. The brightening is seen to propagate along the magnetic loops till ∼19:35 UT, when it reached the northern ends and the entire magnetic loop was brightened. During this time interval, the filament, as well as the brightened TRACE loops, only show limited outward motion, same as what we see in Hα. After ∼19:35 UT, the bright TRACE loops began to erupt outward due to their detachment from the right ends (see 19:38 UT). Simultaneously, the filament shows the rapid eruption as discussed above. Figure 4 shows two TRACE 195 Å images during the eruption process at 19:27 and 19:38 UT, respectively.

4. SUMMARY AND DISCUSSION

The important observational results of this event are as follows: (1) The filament at the boundary of the AR was triggered by the initial flaring near the central δ sunspot, and erupted $\sim$13 minutes after the flare onset; (2) The erupting filament caused a sympathetic flare with moving ribbons at a different site from the initial flare; (3) Brightening was observed to propagate along the large magnetic loops associated with the filament and was co-temporal with the slow rising phase of the filament. Afterward, they erupted outward together.

We want to understand how these sympathetic flares occurred, namely, how the initial flaring triggered the filament eruption in another site. Such process has rarely been reported before and filaments or flux loops may show only oscillations that result from the passage of flare-generated waves (e.g., Liu et al. 2006; Hudson & Warmuth 2004). The disruption of the filament in this event certainly cannot be due to the flare waves generated from the initial flaring, if there was any, since the filament showed no oscillation but slow rising after the flare onset. In this event, the filament as well as the associated large flux loop southeast of the AR have one of their legs rooted at the negative magnetic region, adjacent to the flare kernel C (Figure 2). Right after the initial flare onset, the kernel C extended southward and appeared to heat the adjacent flux loop system there during $\sim$19:24–19:35 UT (see Fig. 4), probably by thermal conduction or ejecting hot chromospheric plasma into the loops. As a result, we see the large loops brightened from the southern ends connecting to the negative fields adjacent to flare patch C. The brightening propagates progressively to the northern ends. Meanwhile, due to the increasing of the temperature, the flux loops became less stable and began to slowly rise outward. Such a thermal nonequilibrium was discussed by Hood and Priest (1981). The filament, probably part of the flux loops, also showed a slow rising during this period. After $\sim$19:35 UT, the whole flux loops were heated and erupted outward rapidly due to the complete loss of equilibrium. This removed the magnetic tension pressing down the filament, which erupted abruptly at this time as well. Therefore, we suggest that the heating of the flux loop system due to the initial flaring destabilized the flux loops and filament, and their final eruption lead to the sympathetic flaring. Alternatively, we may also suggest that the erupting of the bright TRACE loop is due to an unresolved reconnection in the area close to the flare patch C.

A related question is then how the initial flaring was triggered at the first place. We are unsure of the answer but provide several pieces of evidence that may offer some insight. First, the RHESSI X-ray loop observation shows the interaction of initial flaring loops AD and BC (see Fig. 2). Second, same as what we found for a number of other events (Wang et al. 1994, 2004; Liu et al. 2005), the new connectivity across the neutral line of the kernels A–B is detected. Figure 5 plots the mean transverse field as the function of time for that section of the neutral line. We survey the entire field of view, only the section of neutral line marked by the black box in Figure 1 (1933 UT) shows obvious change in transverse field strength: increasing from 820 G to 1050 G,

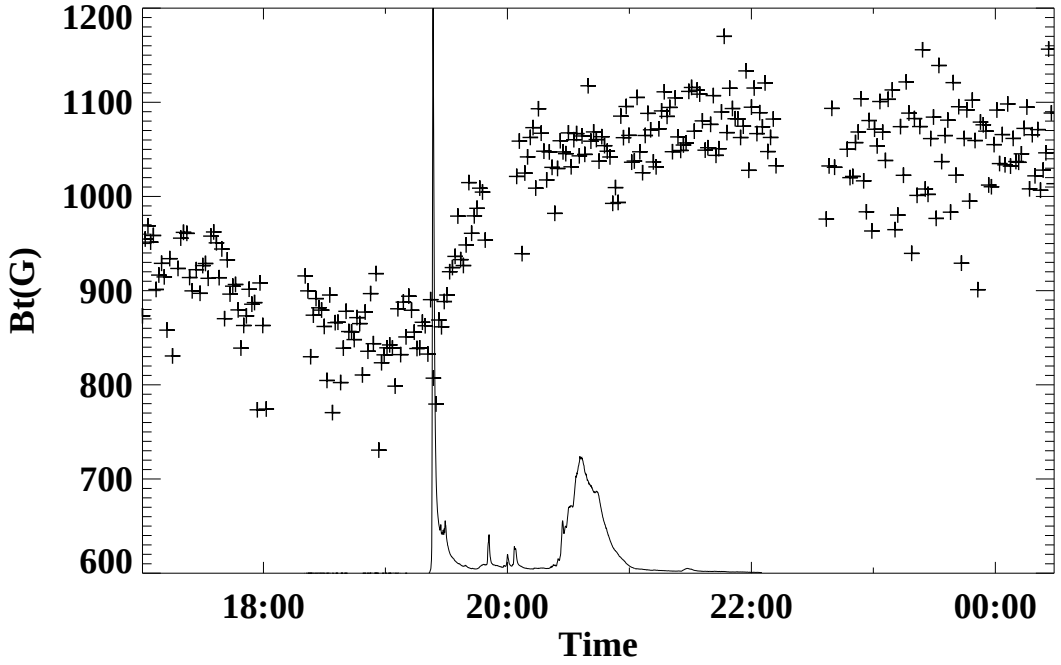

Fig. 5.— The time profile of the mean transverse field strength for the area marked by the black box in Figure 1. This is the section of the neutral line close to the initial flare core. The timing of the flare is indicated by the 10 GHz OVSA microwave light curve.

starting immediately as the flare was initiated. Thus, we speculate that the loops AD and BC could have reconnected following the tether-cutting flare model (Moore et al. 2001, and references therein), and thus lead to the separating ribbons 1*a* and 1*b* as well as the new connections between AB. According to that model, after the flare, a short loop should form very close to the solar surface connecting two interacting loops.

The work is supported by NSF under grants ATM 05-36921 and ATM 05-48952, and by NASA under grant NNX07AH78G.

REFERENCES

Birn, J., Forbes, T. G., & Hesse, M. 2006, ApJ, 645, 732

Gary, D. E., & Hurford, G. J. 1990, ApJ, 361, 290

Gopalswamy, N., Nitta, N., Manoharan, P. K., Raoult, A., & Pick, M. 1999, A&A, 347, 684

Handy, B. N., et al. 1999, Sol. Phys., 187, 229

Hood, A.W. & Priest, E.R., 1981, Sol. Phys., 73, 289

Hudson, H. S., & Warmuth, A. 2004, ApJ, 614, L85

Khan, J. I., & Hudson, H. S. 2000, Geophys. Res. Lett., 27, 1083

Kopp, R. A., & Pneuman, G. W. 1976, Sol. Phys., 50, 85

Lin, R. P., et al. 2002, Sol. Phys., 210, 3

Liu, C., Deng, N., Liu, Y., Falconer, D., Goode, P. R., Denker, C., & Wang, H. 2005, ApJ, 622, 722

Liu, C., Lee, J., Deng, N., Gary, D. E., & Wang, H. 2006, ApJ, 642, 1205

Manoharan, P. K., van Driel-Gesztelyi, L., Pick, M., & Démoulin, P. 1996, ApJ, 468, L73

Moon, Y.-J., Choe, G. S., Park, Y. D., Wang, H., Gallagher, P. T., Chae, J., Yun, H. S., & Goode, P. R. 2002, ApJ, 574, 434

Moore, R. L., Sterling, A. C., Hudson, H. S., & Lemen, J. 2001, ApJ, 552, 833

Pearce, G., & Harrison, R. A. 1990, A&A, 228, 513

Shi, Z.-X., Wang, J.-X., & Luan, D. 1997, Acta Astronomica Sinica, 38, 257

Spirock, T. J., Yurchyshyn, V. B., & Wang, H. 2002, ApJ, 572, 1072

Wang, H., Ewell, M. W., Zirin, H., & Ai, G. 1994, ApJ, 424, 436

Wang, H., Chae, J., Yurchyshyn, V., Yang, G., Steinegger, M., & Goode, P. R. 2001, ApJ, 559, 1171

Wang, H., Gallagher, P., Yurchyshyn, V., Yang, G., & Goode, P. R. 2002, ApJ, 569, 1026

Wang, H., Qiu, J., Jing, J., & Zhang, H. 2003, ApJ, 593, 564

Wang, H., Qiu, J., Jing, J., Spirock, T. J., Yurchyshyn, V., Abramenko, V., Ji, H., & Goode, P. R. 2004, ApJ, 605, 931

Wang, H. 2005, ApJ, 618, 1012

Wheatland, M. S., & Craig, I. J. D. 2006, Sol. Phys., 238, 73

Zhang, C., Wang, H., Wang, J., & Yan, Y. 2000, Sol. Phys., 195, 135